Independent Movement of the Regulatory and Catalytic Domains of Myosin Heads Revealed by Phosphorescence Anisotropy†

Louise J. Brown,‡ Nicholas Klonis,§ William H. Sawyer,§ Peter G. Fajer,|| and Brett D. Hambly*,‡

Department of Pathology, University of Sydney NSW 2006, Australia, Russell Grimwade School of Biochemistry and Molecular Biology, University of Melbourne, Parkville 3052, Australia, and The National High Magnetic Field Laboratory, Institute of Molecular Biophysics, and Department of Biological Science, Florida State University, Tallahassee, Florida 32306

Received March 21, 2001; Revised Manuscript Received May 9, 2001

ABSTRACT: Inter- and intradomain flexibility of the myosin head was measured using phosphorescence anisotropy of selectively labeled parts of the molecule. Whole myosin and the myosin head, subfragment-1 (S1), were labeled with eosin-5-iodoacetamide on the catalytic domain (Cys 707) and on two sites on the regulatory domain (Cys 177 on the essential light chain and Cys 154 on the regulatory light chain). Phosphorescence anisotropy was measured in soluble S1 and myosin, with and without F-actin, as well as in synthetic myosin filaments. The anisotropy of the former were too low to observe differences in the domain mobilities, including when bound to actin. However, this was not the case in the myosin filament. The final anisotropy of the probe on the catalytic domain was 0.051, which increased for probes bound to the essential and regulatory light chains to 0.085 and 0.089, respectively. These differences can be expressed in terms of a "wobble in a cone" model, suggesting various amplitudes. The catalytic domain was least restricted, with a 51 ± 5° half-cone angle, whereas the essential and regulatory light chain amplitude was less than 29°. These data demonstrate the presence of a point of flexibility between the catalytic and regulatory domains. The presence of the "hinge" between the catalytic and regulatory domains, with a rigid regulatory domain, is consistent with both the "swinging lever arm" and "Brownian ratchet" models of force generation. However, in the former case there is a postulated requirement for the hinge to stiffen to transmit the generated torque associated by nucleotide hydrolysis and actin binding.

The atomic structure of the myosin head (S1) in its intermediate states has led to a model of muscle contraction where force generation is produced by a conformational change in the catalytic domain of the myosin head during ATP[1] hydrolysis, which results in a rotation of the regulatory domain, acting as a lever arm (*1*, *2*). Implicit in this model is the hypothesis that a point of flexibility, or hinge, is located within the myosin head region, around which the regulatory domain can move with respect to the catalytic domain.

Evidence for nucleotide-induced conformational changes in the myosin head has been provided from transient electrical birefringence and X-ray scattering measurements, where the binding of MgADP and MgADP-vanadate (*3*, *4*) to the S1 head and subsequent ATP hydrolysis (*5*) appeared to make S1 more flexible. EPR, fluorescence, and phosphorescence spectroscopic studies have demonstrated an ordered fraction of catalytic domains during force generation in fibers (*6*), but in the regulatory domain either disorder (*7*, *8*) or the formation of new angular distributions (*9*). Electron microscopic reconstructions of smooth and nonmuscle S1 bound to actin filaments revealed a rotation of the regulatory domain with respect to the catalytic domain upon MgADP binding (*10*, *11*). These results were confirmed by EPR spectroscopy (*12*).

It has been suggested that rotational motions of the myosin head are connected with force generation during muscle contraction. Recent ST-EPR measurements of the catalytic and regulatory domains in myosin filaments, in the absence of nucleotide, have shown that the mobility of the regulatory domain is significantly slower than the catalytic domain, suggesting that the two domains are capable of independent movement via a flexible hinge. However, these data were unable to provide the angle through which this motion occurred (*13*).

This limitation is addressed here by measuring time-resolved phosphorescence anisotropy, which is capable of measuring the rate and amplitude of microsecond motions. This technique has been used successfully to measure mobility of the muscle crossbridges in various states of myosin polymerization and in myofibrils or fibers in various intermediate states of the ATPase cycle (*14*−*21*). These studies have mainly focused on probes attached to Cys 707 of the catalytic domain.

† Research sponsored by NHMRC and National Heart Foundation of Australia, National Science Foundation NSF-IBN-9808708, NHMFL IHRP 5024 and the American Heart Association GIA-9950424N.

* To whom correspondence should be addressed. E-mail: bretth@pathology.usyd.edu.au.

‡ Department of Pathology.

§ Russell Grimwade School of Biochemistry and Molecular Biology.

|| The National High Magnetic Field Laboratory.

[1] Abbreviations: ADP, adenosine 5′-diphosphate; ATP, adenosine 5′-triphosphate; DMF, *N*,*N*′-dimethyl formamide; DTT, dithiothreitol; E-5-IA, eosin-5-iodoacetamide; EDTA, ethylenediamine tetraacetic acid aminoethyl ether; ELC1, skeletal myosin essential light chain, A1 isoform; ELC2, skeletal myosin essential light chain, A2 isoform; MOPS, 3-(N-morpholino)propane-sulfonic acid; RLC, skeletal myosin regulatory light chain 2; RLC−C125R, recombinant myosin regulatory light chain, with only one cysteine at position 154; S1, myosin subfragment 1; Tris, tris(hydroxymethyl)-aminomethane.

10.1021/bi010566f CCC: $20.00
Published on Web 06/22/2001

In this study, phosphorescence anisotropy was measured in three myosin forms (S1, monomeric, and filamentous myosin) using probes on the ELC, RLC, and the catalytic domain of myosin. The phosphorescent probe, eosin-5-iodoacetamide (E-5-IA), was covalently attached to three sites within the myosin head of intact myosin or to two sites on α-chymotryptic S1. The phosphorescence anisotropy of the probes on these sites indicated that *(a) the catalytic and regulatory domains move independently, and (b) that the regulatory domain moves as a rigid body*.

MATERIALS AND METHODS

Proteins and Chemical Reagents. All procedures were carried out at 4 °C unless otherwise noted. Rabbit skeletal muscle myosin was prepared by the method of Tonomura et al. (*22*). Subfragment-1 (S1) was prepared from myosin by the method of Weeds and Taylor (*23*) and separated into the isozymes S1(A1) and S1(A2) using SP-Sepharose ion-exchange chromatography (*24*). S1 was concentrated, prior to labeling and the exchange reaction, by ammonium sulfate fractionation at 60% saturation. S1(A1) was used for the direct labeling of SH1 and S1(A2) was prepared for the exchange with labeled skeletal myosin essential light chain 1 (ELC1).

ELC1 was isolated from myosin by guanidine-HCl denaturation, followed by ethanol precipitation, using the method of Wagner (*25*), and separated from the other light chains using Cibacron Blue affinity chromatography. Recombinant RLC-C125R, where Cys 125 was replaced by an Arg, leaving only Cys 154, was prepared as described by Boey et al. (*26*).

Rabbit skeletal muscle actin was prepared from acetone powder by the method of Spudich and Watt (*27*), as modified by Barden and dos Remedios (*28*). Before use, freeze-dried monomeric actin was resuspended in G-actin buffer (0.2 mM ATP, 0.1 mM $CaCl_2$, and 20 mM Tris-HCl, pH 8.0) at between 2 and 5 mg/mL and dialyzed against the same buffer for 2 h. G-actin was polymerized to F-actin, by the addition of $MgCl_2$ to 2 mM and KCl to 100 mM, and allowed to polymerize for 1.5 h at 22 °C, before dialysis against phosphorescence buffer (300 mM KCl, 2 mM $MgCl_2$, and 20 mM Tris-HCl, pH 8.0) to remove free ATP.

Glucose oxidase was obtained from Boehringer Mannheim (Indianapolis, IN). The phosphorescent probe eosin-5-iodoacetamide (E-5-IA) was obtained from Molecular Probes (Eugene, Oregon).

Phosphorescent Labeling. Stock E-5-IA (~10 mM) was stored at −20 °C in dimethyl formamide (DMF). For all labeling procedures, the probe was added to the protein sample with vortexing in a minimal volume of DMF (final concentration < 1% v/v) to prevent protein denaturation and precipitation. The optimal time to achieve maximal labeling was determined for each sample.

S1(A1) was modified specifically with E-5-IA at the reactive sulfydryl residue SH1 (Cys 707). Purified S1(A1) (~5 mg/mL) was dialyzed into SH1 labeling buffer (0.15 M KCl and 50 mM TES, pH 8.0) and labeled for 30 min with a 4-fold molar excess of E-5-IA at 4 °C, followed by excess probe removal on a Sephadex G-25 size exclusion column and dialysis against Phosphorescence buffer. Samples were used for TPA experiments within 3 days.

Cys 177 of ELC1 was modified specifically with E-5-IA. ELC1 (~5 mg/mL) was incubated for 30 min at 40 °C in reducing buffer (6 M Gdn-HCl, 10 mM DTT, 2 mM EDTA, and 50 mM Tris-HCl, pH 8.0) to ensure complete reduction of all sulfydryl residues, followed by equilibration in ELC labeling buffer (0.1 mM DTT, 2 mM EDTA, and 50 mM Tris-HCl, pH 8.0) using G-25 chromatography and a 2 h dialysis. The sample was labeled with a 3-fold molar excess of E-5-IA for 4 h at 22 °C, followed by excess probe removal on a G-25 size exclusion column and dialysis against ELC labeling buffer. Samples were freeze-dried for storage.

Cys 154 of recombinant RLC-C125R was reduced with DTT and labeled essentially as described for ELC1, but in the presence of 100 mM NaCl. A 4-fold molar excess of E-5-IA was added and allowed to react overnight at 4 °C. Following excess probe removal, labeled RLC-C125R was freeze-dried for storage.

The reactive sulfydryl residue SH1 (Cys 707) was labeled in myosin according to the method of Eads and Thomas (*14*). Myosin filaments in filament buffer (120 mM KCl, 5 mM $MgCl_2$, 1 mM NaN_3, 1 mM EGTA, and 25 mM MOPS, pH 7.0), containing 4 mM potassium pyrophosphate, were incubated with an 8-fold molar excess of E-5-IA to myosin heads for 30 min at 4 °C, before dissolving the myosin filaments by the addition of 0.17 × volume of 3.0 M KCl, 14 mM DTT, and 10 mM MOPS, pH 7.0 to a final concentration of 0.62 M KCl and 2.4 mM DTT. Unreacted dye was removed using G-25 chromatography equilibrated in 0.6 M KCl, 2 mM EDTA, and 10 mM MOPS, pH 7.0, followed by dialysis against a 50 × volume of 1 mM EDTA and 10 mM MOPS, pH 7.0, to reform the myosin filaments. Following sedimentation, myosin was redissolved in 0.5 M KCl, 0.1 mM EDTA, and 10 mM MOPS, pH 7.0, to 10 mg/mL before centrifuging to clarify at 40000*g* for 30 min. Myosin-SH1* was stored in 50% glycerol at −20 °C.

Actin was labeled by the method of Sawyer et al. (*29*), with modifications outlined by Ludescher and Liu (*18*). Essentially, F-actin (2 mg/mL) was dialyzed against 0.2 mM $CaCl_2$, 2 mM $MgCl_2$, 0.2 mM ATP, 0.1 M KCl, 0.002% NaN_3, and 2 mM Tris-HCl, pH 8.0. A 2-fold molar excess of E-5-IA was added and incubated for 3 h at 22 °C, followed by sedimentation at 150000*g* for 1.5 h and dialysis against 0.2 mM $CaCl_2$, 0.2 mM ATP, 0.002% NaN_3, and 2 mM Tris-HCl, pH 8.0, for 24 h to remove unreacted dye and to depolymerize the actin. The labeled actin monomer sample was then applied to a G-25 size exclusion column, followed by a further cycle of polymerization and depolymerization to ensure complete removal of residual probe.

The labeling stoichiometries of modified proteins were determined by measuring the bound probe concentrations spectrophotometrically using an extinction coefficient of 8.3×10^4 M^{-1} cm^{-1} at 539 nm for E-5-IA (*14*). Protein concentrations were determined using the BCA protein assay (Pierce, Rockford, IL).

Light Chain Exchanges. Phosphorescent-labeled ELC1 was exchanged onto α-chymotryptic S1(A2), as outlined by Wagner and Weeds (*30*), but at a higher pH of 9.5 (*31*). Exchange against S1(A2) maximized the separation of the exchanged and labeled S1(A1) fraction from the unlabeled S1(A2) fraction, using cation exchange chromatography. Freshly cut S1(A2) (40 mg), plus a 5-fold molar excess of freeze-dried labeled ELC1, were dialyzed into exchange buffer (2 mM EDTA, 2 mM DTT, 0.1 M imidazole, pH 7.0). The exchange reaction was initiated by the addition of NH_4-

Cl to 4.7 M. The pH was adjusted to 9.5 with 30% ammonia, followed by a 20 min incubation at 4 °C. NH_4Cl was removed by G-25 chromatography and dialysis overnight against 0.25 mM DTT and 15 mM MOPS, pH 7.0. Free light chains and the two isozymes of S1 were separated using an SP-Sepharose cation exchange column equilibrated in the same buffer and eluted with a linear gradient from zero to 0.22 M NaCl. The exchange product [S1(A1)-ELC1*] was dialyzed against Phosphorescence buffer and concentrated using a Centricon-10 10000 MW cutoff spin column. The exchanged S1 was used for TPA measurements within 3 days.

Exchange of labeled ELC1 (Cys 177) into myosin was accomplished according to the method of Wagner (*25*). A total of 15−20 mg/mL myosin in 0.6 M KCl and 20 mM MOPS, pH 7.0, plus a 14-fold molar excess of freeze-dried labeled ELC1 was dialyzed into exchange buffer (0.3 M KCl, 2 mM EDTA, and 0.1 M MOPS, pH 7.0) and Mg-ATP, DTT, and NH_4Cl added to final concentrations of 5 mM, 0.1 mM and 4.7 M, respectively. The exchange reaction proceeded for 30 min at 4 °C, followed by dialysis against four changes of 100 × volume of 40 mM KCl, 1 mM NaN_3, and 10 mM MOPS, pH 7.0. The precipitated myosin filaments were sedimented at 12000*g* for 20 min, dissolved in 0.6 M KCl and 20 mM MOPS, pH 7.0, and subjected to a second cycle of precipitation and solubilization to remove residual free light chains. Myosin-ELC1* was stored in 50% glycerol at −20 °C.

Labeled RLC-C125R was exchanged onto myosin by incubating a 10−20-fold molar excess of RLC over myosin (*32*). Approximately 5 mL of labeled RLC-C125R (5 mg/mL) was dialyzed into RLC exchange buffer (0.5 M NaCl, 2 mM DTT, 2 mM EDTA, and 40 mM Tris-HCl, pH 8.0). Myosin (20 mg; final concentration ≈ 1.2 μM) in exchange buffer was added to the light chains to a final concentration of ∼0.5 mg/mL (final concentration ≈ 25 μM). MgATP was added to a final concentration of 5 mM and the mixture was incubated at 37 °C for 10 min. The solution was then immediately cooled on ice and $MgCl_2$ added to 10 mM, followed by a 10 min incubation. The exchange mixture was precipitated with 14 vol of 1 mM $MgCl_2$ and 5 mM MOPS, pH 7.0 for 30 min, sedimented at 12000*g* for 10 min and redissolved in 0.6 M KCl and 5 mM MOPS, pH 7.0. A second precipitation and resuspension cycle was performed to ensure removal of all free light chains. The final myosin-RLC* labeled exchange product was dissolved in Phosphorescence buffer and stored in 50% glycerol at −20 °C.

Phosphorescence Anisotropy Measurements. The custom-built phosphorescent apparatus and measuring procedures for the anisotropy decay measurements have been described previously (*29*). Deoxygenated samples in a quartz cuvette were excited by vertically polarized light at 515 nm with an 8−10 ns pulse width from a coumarin dye laser (Molectron DL 10/14) driven by a pulsed nitrogen laser (Molectron UV 14, 1 mJ/pulse, 20 Hz). Phosphorescence emission was isolated using a combination of RG695 and KV550 Schott cutoff filters. To avoid the intense spike of prompt fluorescence, a gated photomultiplier was used to measure the phosphorescence 1 μs after the laser pulse.

Decays of the parallel [$I_{VV}(t)$] and perpendicular [$I_{VH}(t)$] components of the polarized transient phosphorescence were collected over the time period 4−800 μs by the 90° rotation of the emission polarized filter after the collection of each set of 64 decays. A total of 512 decays (minimum of 8 decay sets) of each vertical and horizontal component were accumulated, digitized and averaged by a 1024 channel signal averager. A minimum of triplicate data sets was collected for each sample.

The background signal was automatically subtracted, and decays were transferred to a computer. Spectra were corrected for drift in the intensity of the vertically polarized light by monitoring the intensity of the excitation light during the measurement. Data collected prior to 4 μs were distorted due to jitter in the gating circuitry and hence discarded. Data were analyzed using custom-written software (DAOS; Labsoft Associates, Melbourne, Australia). Decays were fitted using a nonlinear least-squares iterative procedure based on the Cheybyshev transformation procedure, which was part of the data acquisition operating system (*29*).

Steady-state phosphorescence anisotropy measurements were made using a Perkin-Elmer LS50B fluorimeter equipped with a Xe flash lamp and a gated delay to collect the phosphorescence. The myosin monomer labeled samples were excited at 480 nm using 15 nm slit width, the emission intensity monitored at 690 nm with a 20 nm slit width. Intensities were collected using an initial time delay of 0.05 ms to avoid any delayed fluorescence or motional effects and integrated over a 1 ms time window. The vertically (I_{VV}) and horizontally (I_{VH}) polarized light was used in the calculation of the steady-state anisotropy according to the following equation:

$$r = (I_{VV} - GI_{VH})/(I_{VV} + 2GI_{VH}) \quad (1)$$

where G is an instrumental correction factor correcting for the ratios of the sensitivities of the detection system for vertically and horizontally polarized light. $r(o)$ was estimated from a Perrin plot (eq 2) of the steady-state anisotropy as a function of solvent viscosity (induced by the addition of a saturated sucrose solution in the appropriate buffer) (*33*). Sucrose was added over the range of 10−30% (wt/wt) at 4 °C and the conditions varied the viscosity from 2.073 to 5.422 cP.

$$1/r = 1/r(o) + (k_B\tau T/r(o)V\eta) \quad (2)$$

η is the viscosity of the solution, k_B is the Boltzmann constant, τ is the phosphorescence lifetime, T is the absolute temperature, and V is the effective hydrodynamic volume of the spherical protein. The viscosity of sucrose solutions was obtained from (*34*). A plot of $1/r$ versus T/η is linear for isotropic motion with an ordinate intercept corresponding to $r(o)$.

Phosphorescence anisotropy curves were used to calculate the cone-half-angle (θ_c) by analyzing the phosphorescence anisotropy in terms of an isotropic rotational model to estimate the average angular displacement of the probe, using the model of Kinosita (*35*, *36*). θ_c was calculated from the initial $r(o)$ and final $r(\infty)$ anisotropy values using the following equation:

$$\frac{r(\infty)}{r(o)} = [0.5 \cos \theta_c(1 + \cos \theta_c)]^2 \quad (3)$$

This model has been applied to the case of a lipid molecule

Table 1: Protein Characterization: The Efficiency of Exchange of Light Chains onto Myosin and the Final Protein Labeling

sample	exchange efficiency (%)	final protein label (mol:mol)
S1(A1)-SH1*		0.9−1.0
S1(A1)-ELC1*	40−60	0.9−1.0[a]
Myosin-SH1*		0.95−1.1
Myosin-ELC1*	50−60	0.45−0.5
Myosin-RLC*	40−60	0.35−0.55
F-actin*		0.95−1.05

[a] S1(A1)-ELC1* fraction purified by chromatography.

wobbling about the bilayer normal and can equally successfully be applied to segmental motion within a protein that satisfies the symmetry requirements, for example, myosin head motion.

All phosphorescence measurements on protein samples were undertaken in Phosphorescence buffer at 12 °C, except the three phosphorescent-labeled myosin filament samples, which were prepared by dialysis of the corresponding labeled myosin monomer sample against 100 × volume of Myosin Filament buffer (120 mM KCl, 5 mM $MgCl_2$, 1 mM NaN_3, 1 mM EGTA, and 25 mM MOPS, pH 7.0) for 8 h. Measurements for S1 and myosin monomer labeled samples were performed in both the presence and absence of unlabeled F-actin. For measurements in the presence of F-actin, labeled S1 and myosin samples were incubated with F-actin for at least 1 h at 22 °C. Sedimentation binding studies confirmed that greater than 95% of S1 and myosin was bound to F-actin under these conditions.

Oxygen must be removed from the phosphorescence samples before spectroscopic measurement to eliminate photobleaching that can degrade the phosphorescence signal intensity by triplet-state quenching by oxygen. Oxygen was enzymatically removed from all phosphorescence samples by the addition of glucose oxidase (30 μg/mL), glucose (45 μg/mL), and catalase (20 μg/mL). Samples were placed in a 7 × 7 mm cross-section cuvette, and the surface of the sample was flushed continuously with argon for 15−20 min prior to phosphorescence data collection to maintain the oxygen-free environment. The protein concentrations were adjusted to the final probe concentration of 1−2 μm to avoid *inner filtering* effects.

RESULTS

Sample Characterization. All proteins were labeled with high efficiency (Table 1) and, in the case of SH1, with high specificity, as shown in Figure 1. A labeling ratio of ∼90% was achieved for SH1, with less than 5% of the probe on the myosin light chains. In the case of the light chains, which each contain a single cysteine, >90% of sulfydryls were modified.

The separation of the exchanged S1(A1)-ELC1* from unexchanged S1(A2) and free ELC1*, using SP-Sepharose cation exchange chromatography is shown in Figure 2. The SDS−PAGE gel shows that the void peak (peak A, lane 2) contained free ELC (both ELC1* and ELC2). Peak B (lane 3) eluted near the beginning of the salt gradient (0 to 0.22 M NaCl) and contained unmodified S1(A2), plus contamination with free ELC1*, while peak C (lane 4) contained the exchanged S1(A1)-ELC1* and was well separated from the other peaks. Note that the proportion of S1 that exchanged

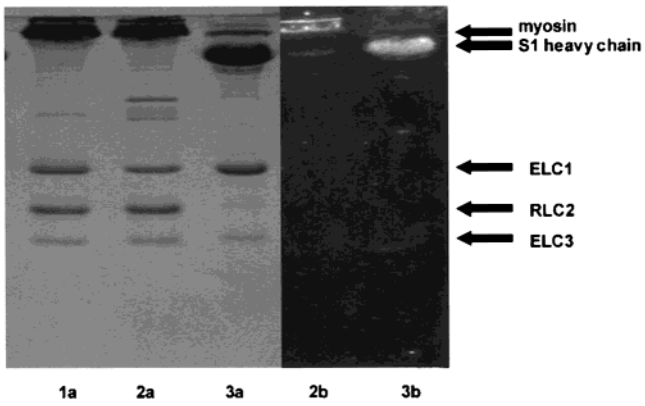

FIGURE 1: SDS−PAGE (16%) of unlabeled myosin control (lane 1); eosin labeled myosin (lane 2) and labeled S1 (lane 3). (Left, a) Coomassie blue; (right, b) UV illuminated gel.

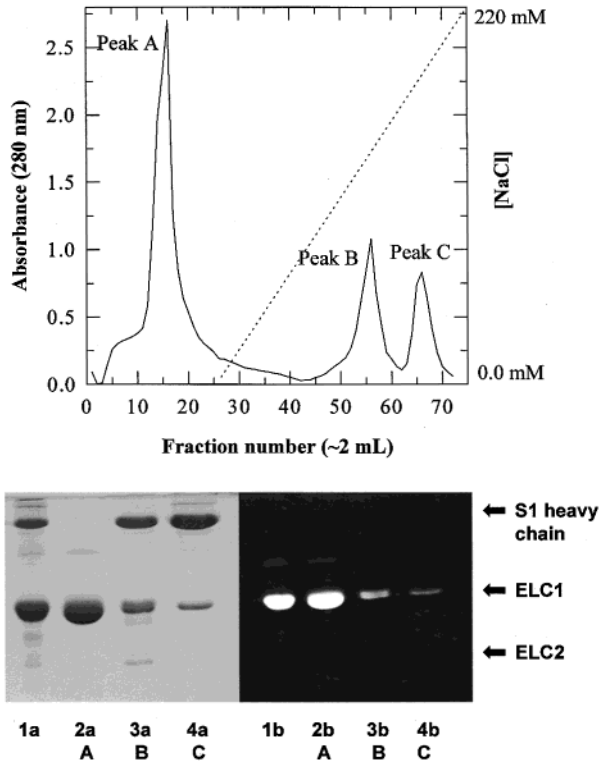

FIGURE 2: Exchange of ELC1* with S1(A2). (Top) Elution profile of the exchange of S1(A2) with ELC1* using SP−Sepharose chromatography, flow rate 2 mL/min. Salt gradient, dotted line. (Bottom) SDS−PAGE (16%) of corresponding peaks A, B, and C from chromatogram. (a) Coomassie blue stain. (b) UV illumination. Lane 1, exchanged sample prior to chromatography; lane 2, peak A free light chains, lane 3, peak B unexchanged S1(A2) with contaminating ELC1*; lane 4, peak C purified exchange product S1(A1)-ELC1*.

was approximately 50%, while the S1(A1)-ELC1* final protein product achieving 90−100% labeling, Table 1.

The efficiency of exchange in myosin of both RLC and ELC was between 40 and 60%, with the final protein product achieving 35−55% labeling, Table 1. Incubation of the myosin with the labeled RLC at 37 °C was kept to a minimum (∼10 min) so as not to denature the myosin (*32*). Following exchange with either of the light chains, myosin was twice cycled through precipitation-resuspension steps to ensure complete removal of free labeled light chains.

Phosphorescence Anisotropy. (1) S1, Soluble Myosin, Actin and Their Complexes. Current models of force generation

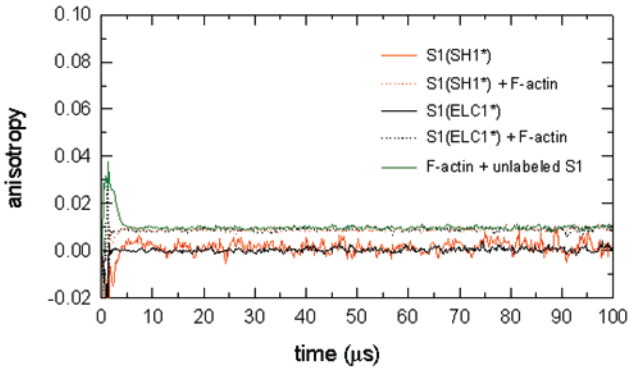

FIGURE 3: Phosphorescence anisotropy of S1 labeled at either SH1 (catalytic domain) or ELC1 (regulatory domain) in the absence (red and black solid lines, respectively) or presence (red and black dotted lines, respectively) of F-actin. TPA curve of labeled F-actin in the presence of unlabeled S1 (green).

imply that a flexible hinge may exist between the catalytic and regulatory domains of the myosin head (*2*). To test this hypothesis, phosphorescence anisotropy measurements were performed for probes bound to either the catalytic or regulatory domains of subfragment 1 (S1) in the presence and absence of F-actin.

The time-resolved phosphorescence anisotropy data for S1 labeled at the catalytic domain (SH1) and the regulatory domain (ELC1) in the absence of F-actin are shown in Figure 3 (ignore the initial 4 μs). As expected, the anisotropy of both domains in solution was close to nil, consistent with previous results (*14*). This suggests that the rotation is essentially isotropic in solution, due to expected rapid tumbling motion of the whole S1 molecule.

S1 binding to F-actin has been previously shown to restrict probe motion when the probe is bound to SH1 in myosin and S1 (*14*). Measurements in the presence of F-actin were performed with a molar ratio of S1:F-actin monomer of 0.6: 1.0 in nucleotide free buffer. Upon the addition of F-actin, there was a small increase in the final anisotropy, $r(\infty)$, for both catalytic and regulatory domains in the acto-S1 complex, Figure 3. This increase in higher final anisotropy values generally indicates more restricted mobility. The final anisotropy values were between 0.0 and 0.01, implying motional restriction induced upon F-actin binding, Figure 4. However, the experimental errors mask differences in motion of the catalytic and regulatory domains in the actoS1 complex.

Similar results to those for S1 were observed for myosin monomers. A summary of these data are shown in Figure 4. In the absence of F-actin, the phosphorescence emission of eosin from all three labeled sites on the myosin head were essentially depolarized and independent of time in the range of 4−800 μs. The final anisotropy decayed to approximately zero, consistent with the range of rotation of the myosin monomer being essentially unrestricted on the microsecond time scale. The decay of the anisotropy was largely complete within the first 4 μs, precluding the calculation of rotational rates.

F-actin was added to each myosin monomer sample to a ratio of myosin to F-actin monomer of 0.3:1.0. Upon the addition of F-actin, the final anisotropy $r(\infty)$ for the probe located on the catalytic domain increased to 0.024 ± 0.011. The anisotropy of probes located on ELC1 and RLC in the

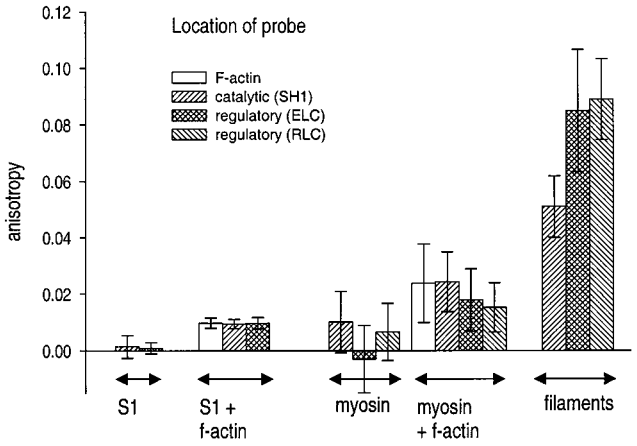

FIGURE 4: Summary of final anisotropy values $r(\infty)$. Bar chart showing the comparison between the final anisotropy values $r(\infty)$ ± SD, for both the catalytic and regulatory domains of myosin in either S1 ± F-actin, myosin ± F-actin or in myosin filaments. $r(\infty)$ was determined by averaging the anisotropy values from 10 to 100 μs.

regulatory domain increased to 0.018 ± 0.011 and 0.015 ± 0.009, respectively. As for acto-S1 the differences are within the experimental error and are consequently statistically insignificant.

To measure the contribution of actin mobility to the observed anisotropy of myosin, we have measured the phosphorescence anisotropy of eosin attached to Cys 374 of actin. Actin $r(\infty)$ in the acto-S1 complex was found to be similar (<0.01) to the values obtained for samples labeled at SH1 and ELC1. In complexes with myosin, actin probe anisotropy increased to 0.024 ± 0.014, as it did for probes bound to sites on myosin. These results suggest that the anisotropy values observed for probes bound to the catalytic and regulatory domains of S1 and myosin are determined by the motion of the F-actin/myosin complex, as expected for a rigid complex.

(2) Myosin Filaments. In the filamentous form, myosin is a mega Dalton complex with the filament backbone completely immobilized on the millisecond time scale. This allows us to measure segmental domain motion otherwise inaccessible in the monomeric form, due to fast, microsecond mobility of the whole soluble protein.

The phosphorescence anisotropy of eosin probes bound to the catalytic domain (SH1) and the regulatory domain (ELC1 or RLC) of filamentous myosin are shown in Figure 5. As expected, the residual anisotropies observed for all the probes sites on filamentous myosin were substantially greater than those observed for the same site in myosin monomers or in S1, in agreement with the original findings of Mendelson (*37*) and Thomas (*38*) for probes on SH1.

Importantly, the differences in final anisotropy are clearly defined, Figure 4. For the catalytic domain, $r(\infty) = 0.051 \pm 0.011$; for the regulatory domain, the final anisotropy of the probe on ELC1 was 0.085 ± 0.022 and for RLC 0.089 ± 0.010. Higher anisotropy for probes on the essential and regulatory light chains, imply greater motional restriction in comparison to the catalytic domain, consistent with the proposed hinge between the two domains (*13*, *39*). Notably, the anisotropy of the proximal and distal parts of the regulatory domain (ELC and RLC, respectively) was the same, suggesting little, if any, relative flexibility of the two halves of the domain.

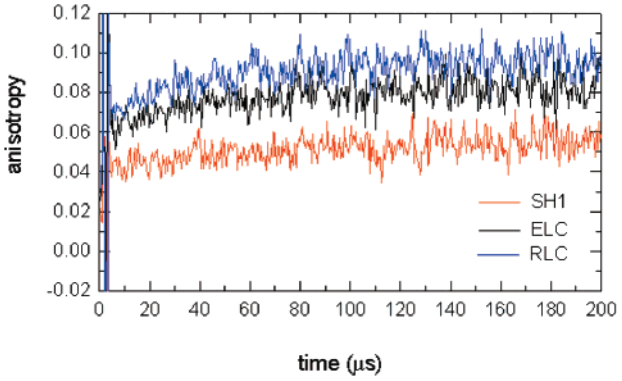

FIGURE 5: Phosphorescence anisotropy of myosin filaments labeled at SH1 (red), ELC1 (black), or RLC−C125R (blue).

Fitted final anisotropy values were within 10% of the calculated average $r(t)$ in the 700−800 μs time range, indicating that the decay reached a plateau level within the analyzed time window. A small rise in the anisotropy was observed for the filament data in rigor between approximately 10−100 μs. This rise was small but reproducible between experiments and preparations. It has been observed by others in filaments labeled at SH1 in rigor and has been explained to be a consequence of the "heterogeneous lifetimes of the eosin probe" (*19*). If a short-lifetime component has a slightly smaller constant value for the anisotropy than a longer lifetime component, then the changing weighted average of the two components will give a rising anisotropy (*20*).

(3) Cone Model of Motion. The depolarization of the emitted light can be related to the half-cone angle θ_c through which the probe transition dipole can freely rotate according to eq 3. This model was previously used with success to describe the mobility of the catalytic domain in filaments and within the myofilament lattice (*15*, *16*, *19*). Calculation of the cone angle of motion requires the determination of the initial anisotropy $r(o)$ in addition to $r(\infty)$.

As most of the decay occurred within the instrumental deadtime on our time-resolved apparatus, steady-state phosphorescence anisotropy was employed to measure the $r(o)$ for each sample. Estimates of the $r(o)$ values were obtained from the extrapolation of the Perrin plots to a zero value of T/η (Figure 6). The values measured for $r(o)$ in the monomer samples were SH1−0.185 ± 009, ELC−0.124 ± 006, and RLC−0.125 ± 0.007. The value obtained for SH1 was in good agreement with a previously obtained value (*19*). Using eq 3, the calculated half-cone angle for the regulatory domain is 28.6 ± 9° for ELC and 26.6 ± 6° for RLC, as compared to 51 ± 5° for the catalytic domain, Figure 7. These angular distributions for the catalytic and regulatory domains of myosin differ by a factor of approximately 1.5−2.

These results provide support for the presence of an internal hinge, or region of flexibility, within the myosin head between the catalytic and regulatory domains. Additionally, the lack of a significant difference between the half cone angles for the essential and regulatory light chains is consistent with the regulatory domain behaving as a rigid body.

DISCUSSION

The mobility of various domains of the myosin head was measured using the phosphorescence anisotropy of eosin. The three targeted sites were Cys 707 of the catalytic domain, Cys 177 of ELC1, and Cys 154 of RLC. Mobilities were determined for S1, soluble myosin, myosin in the actomyosin complex and in synthetic myosin filaments. The residual anisotropy in myosin filaments was greater for all sites than for monomeric myosin or S1, consistent with the higher degree of motional restriction following filament assembly. More importantly, the mobility measured in filaments for the catalytic domain was greater than for the two sites within the regulatory domain. In terms of the *wobble in a cone* model (*40*), the catalytic domain possesses a greater motional amplitude (half-cone angle of 51 ± 5°) compared to the regulatory domain (half-cone angle of <29°). This finding implies independent mobility of the two domains, suggesting a hinge between the catalytic and regulatory domains. By contrast, the mobility of the ELC is the same as the mobility of the RLC, demonstrating the

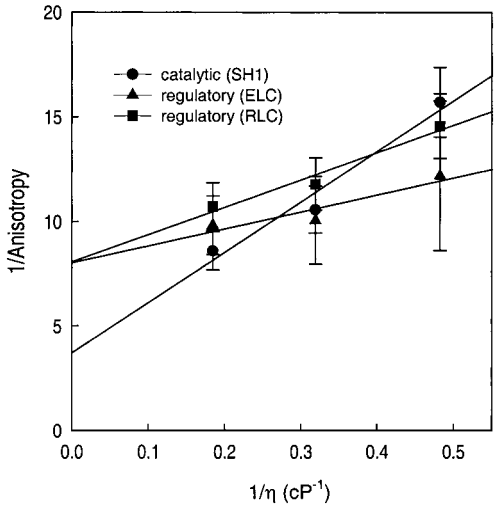

FIGURE 6: The effect of solution viscosity (η) on the phosphorescence emission anisotropy (±SE) of eosin-labeled sites [SH1 l (●), ELC (▲), and RLC (■)] on the myosin monomer. Solution viscosity was modulated by adding sucrose to the sample at 4 °C. Data were plotted using a simplified Perrin equation (see Materials and Methods).

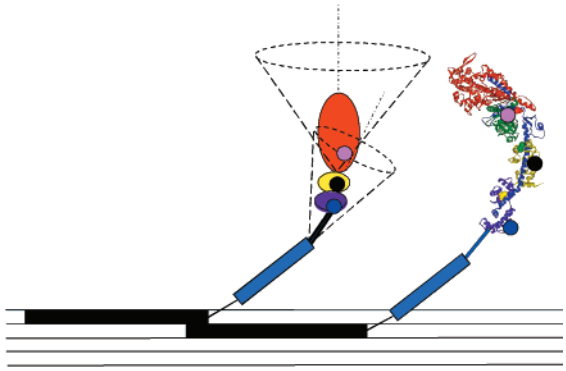

FIGURE 7: Schematic model of myosin head motion. The estimated half-cone angle for the catalytic (red) and regulatory domains (yellow-ELC, purple-RLC) in filaments. The catalytic domain amplitude is 51 ± 5° and the regulatory domain is 29 ± 8° (28.6 ± 9° for ELC and 26.6 ± 6° for RLC). The approximate location of the probes at SH1 (catalytic), Cys177 (ELC1), and Cys154 (RLC−C125R) are represented by pink, black and blue circles, respectively. S2 is represented by the blue bar that links the head to the myosin thick filament (black). The cones of motion are drawn to emphasize the difference between the catalytic and regulatory domains.

absence of detectable flexibility in the regulatory domain.

An indication of flexibility between the catalytic and regulatory domains was recently reported (*13*) using EPR techniques, although these data are effective correlation times, which represent a composite of the rotational rate and limiting angle of rotational motion. If we combine the ST-EPR and TPA data, we dissect the rate and amplitude of domain motions and show that the mobilities differ primarily in the amplitude. In ST-EPR, fast motions with small amplitude result in spectra similar to those of slow motions with larger amplitude. TPA is capable of differentiating between the rate and amplitude, thus allowing us to characterize more fully the motion at this hinge. Although, we have not been able to measure the rate directly, our estimates for amplitude of motion can be used to obtain the rotational rates from the previously published ST-EPR data. According to computational simulations (*41*), a change of amplitude of motion from 29° to 51°, measured here using TPA, results in a 1.5-fold decrease in effective correlation time. Thus, the observed 3-fold difference in effective correlation times measured by ST-EPR (*13*, *39*) can at most correspond to 2-fold difference in the rate of motion, i.e., if the catalytic domain correlation time is $\tau_r = 7$ μs then the correlation time for the regulatory domain would be 14 μs.

Relationship to Other Studies: The Converter Region. Reorientation between the two domains of the myosin head has been postulated by Huxley (*42*) and more recently by Highsmith and Cooke (*43*). The evidence for such a model has been more difficult to obtain but definite shape changes of the myosin head have been experimentally observed. For example, electric birefringence (*3*), neutron diffraction (*44*), electron microscopy (*11*, *45*), and distance measurements by FRET (*46*−*49*) as well as the various crystal structures (*50*) all show changes in the conformation of the isolated myosin head. More importantly and of physiological relevance, similar changes have been observed in muscle fibers using (a) electron paramagnetic resonance spectroscopy, showing different orientational distributions of the catalytic and regulatory domains (*7*, *9*) and (b) different fluorescence anisotropy between the domains (*51*, *52*).

The point of dynamic flexibility implied by the above studies requires direct experimental localization. The filament data in this work has localized the point of flexibility within the myosin head to the region that lies between the SH1 site (Cys 707) and the ELC1 site (Cys 177). This region, often referred to as the converter domain, represents a very small section of the length of the myosin head and specifically includes the interface between the 25 kDa domain and the ELC (*1*, *53*). Several mutagenesis studies of key residues located in the converter domain and the two conserved glycine residues (709, 720) have emphasized the importance of the conformational changes thought to occur in this region during the contractile cycle (*54*−*56*). A large number of Familial Hypertrophic Cardiomyopathy (FHC) mutations have been found in a cluster at the interface between the 25 kDa domain and the carboxy-terminal portion of the ELC and also reflect the importance of this region. Several of these FHC mutations uncoupled force generation from the ATPase activity (*57*, *58*). Comparison of crystal structures of S1, with various bound nucleotide analogues, suggest that the regulatory domain is rotated by a large angle in comparison to its location in the skeletal S1 structure in the absence of nucleotides (*50*, *53*, *59*). A mechanism based on rearrangement of the catalytic, converter, regulatory and SH3 domains, connected by several joints, has been proposed by Cohen and collaborators to affect this motion of the regulatory domain (*50*). A reversal of the movement of an unconventional myosin VI, which allows a putative lever arm to rotate in the opposite direction to conventional myosin, reinforces the "swinging lever arm" model (*60*).

The considerable flexibility observed in this hinge in the absence of bound nucleotide and actin, suggests that for force to be generated this hinge needs to stiffen considerably. A model of force generation has been proposed where the myosin head undergoes a disorder to order transition following hydrolysis of ATP and actin binding (*61*−*63*). A crucial element of such a model is stiffening of the myosin head across its length during force generation.

A recent phosphorescence study in a chimera of scallop myofibrils, using chicken gizzard regulatory light chain labeled at Cys 108, revealed a 2-fold less restricted mobility than observed here (*64*). No comparative data for the scallop catalytic domain are available, precluding conclusions about the hinge in scallop myosin. The direct comparison with the rabbit skeletal catalytic domain, which has similar amplitude (*19*), would suggest that protein dynamics in scallop may differ from that in the skeletal isoform.

Intradomain Changes. The motivation for measuring the anisotropy of probes attached to each of the two light chains of myosin was to test whether the regulatory domain behaves as a passive, rigid lever. Highsmith and Eden (*4*) have recently noted a decrease of segmental flexibility in a complete myosin head with RLC present, as compared to a shorter chymotryptic S1 containing only ELC. Additionally, Spudich and Howard postulated that bending of the regulatory domain may store some of the mechanical energy during force generation (*65*).

The data presented here demonstrate no significant difference in mobility between the two halves of the regulatory domain, implying that the domain is rigid, allowing it to act as a lever arm during force generation. While the rigid-lever hypothesis is intuitively logical and generally accepted, the evidence is still the object of research. The strongest support for a rigid lever arm comes from in vitro mobility studies, in which the translocation rate increased with increasing length of the regulatory domain (*66*). However, an argument has been made that the velocity in an in vitro motility assay is determined by the lifetime of the attached state, which may be a function of the regulatory domain. Direct measurement of the stepsize under loaded conditions using scanning probe nanometry revealed the same 5.5 nm step for intact myosin and a mutant lacking the regulatory domain (*67*). Similar measurements of the powerstroke distance, using optical tweezers, for three myosin isoforms containing either two, three or six light chains yielded a ratio of 1:2:2 for the step size distances, leaving open the possibility of intradomain flexibility, especially for longer regulatory domains (*68*). The presence of similar segmental mobility across the length of the regulatory domain does not preclude more static conformational changes between the two light chains. For example, in scallop myosin, Ca^{2+} binding results in increased interaction between the two light chains which might lead to a stiffening of the regulatory domain (*69*). Finally, recent FRET data show that the distance between the ELC and RLC

does not change significantly as a function of myosin state, implying that no significant static reorientation occurs between the two light chains in the pre- and post-powerstroke states (*49*).

In conclusion, the phosphorescence anisotropy data presented here demonstrate a difference in mobility between the catalytic and regulatory domains of the myosin head. This difference is mainly in the amplitude of motion, with the catalytic domain possessing at least 1.5 times the amplitude of the regulatory domain. On the other hand, the two halves of the regulatory domain experience similar restriction of motion, suggesting that the regulatory domain behaves as a rigid body, as expected for a force transforming lever arm.

The presence of a "hinge" between the two domains which allows relative flexibility of the two domains is not inconsistent with the "swinging lever arm" model for force generation, although it would require modulation of hinge stiffness. This may happen on binding to actin and/or as a function of various nucleotide states. However, an alternate model, a "Brownian ratchet", would permit the persistence of significant flexibility between the two domains (*67*, *70*).

REFERENCES

1. Rayment, I., Holden, H. M., Whittaker, M., Yohn, C. B., Lorenz, M., Holmes, K. C., and Milligan, R. A. (1993) *Science 261*, 58−65.
2. Fisher, A. J., Smith, C. A., Thoden, J., Smith, R., Sutoh, K., Holden, H. M., and Rayment, I. (1995) *Biophys. J. 68*, 19s−28s.
3. Highsmith, S., and Eden, D. (1990) *Biochemistry 29*, 4087−93.
4. Eden, D., and Highsmith, S. (1997) *Biophys. J. 73*, 952−8.
5. Wakabayashi, K., Tokunaga, M., Kohno, I., Sugimoto, Y., Hamanaka, T., Takezawa, Y., Wakabayashi, T., and Amemiya, Y. (1992) *Science 258*, 443−7.
6. Fajer, P. G. (1994) *Biophys. J. 66*, 2039−50.
7. Hambly, B., Franks, K., and Cooke, R. (1992) *Biophys. J. 63*, 1306−13.
8. Ling, N., Shrimpton, C., Sleep, J., Kendrick-Jones, J., and Irving, M. (1996) *Biophys. J. 70*, 1836−46.
9. Baker, J. E., Brust-Mascher, I., Ramachandran, S., LaConte, L. E., and Thomas, D. D. (1998) *Proc. Natl. Acad. Sci. U.S.A. 95*, 2944−9.
10. Jontes, J. D., Wilson-Kubalek, E. M., and Milligan, R. A. (1995) *Nature 378*, 751−3.
11. Whittaker, M., Wilson, K. E., Smith, J. E., Faust, L., Milligan, R. A., and Sweeney, H. L. (1995) *Nature 378*, 748−51.
12. Gollub, J., Cremo, C. R., and Cooke, R. (1996) *Nat. Struct. Biol. 3*, 796−802.
13. Adhikari, B., Hideg, K., and Fajer, P. G. (1997) *Proc. Natl. Acad. Sci. U.S.A. 94*, 9643−7.
14. Eads, T. M., Thomas, D. D., and Austin, R. H. (1984) *J. Mol. Biol. 179*, 55−81.
15. Ishiwata, S., Kinosita, K. Jr., Yoshimura, H., and Ikegami, A. (1987) *J. Biol. Chem. 262*, 8314−7.
16. Ishiwata, S., Kinosita, K., Jr., Yoshimura, H., and Ikegami, A. (1988) *Adv. Exp. Med. Biol. 226*, 267−76.
17. Stein, R. A., Ludescher, R. D., Dahlberg, P. S., Fajer, P. G., Bennett, R. L., and Thomas, D. D. (1990) *Biochemistry 29*, 10023−31.
18. Ludescher, R. D., and Liu, Z. (1993) *Photochem. Photobiol. 58*, 858−66.
19. Ludescher, R. D., and Thomas, D. D. (1988) *Biochemistry 27*, 3343−51.
20. Ludescher, R. D., Peting, L., Hudson, S., and Hudson, B. (1987) *Biophys. Chem. 28*, 59−75.
21. Ramachandran, S., and Thomas, D. D. (1999) *Biochemistry 38*, 9097−104.
22. Tonomura, Y., Appel, P., and Morales, M. (1966) *Biochemistry 5*, 515−21.
23. Weeds, A. G., and Taylor, R. S. (1975) *Nature 257*, 54−6.
24. Prince, H. P., Trayer, H. R., Henry, G. D., Trayer, I. P., Dalgarno, D. C., Levine, B. A., Cary, P. D., and Turner, C. (1981) *Eur. J. Biochem. 121*, 213−9.
25. Wagner, P. D. (1982) *Methods Enzymol. 85*, 72−81.
26. Boey, W., Huang, W., Bennets, B., Sparrow, J., dos Remedios, C. G., and Hambly, B. (1994) *Eur. J. Biochem. 219*, 603−10.
27. Spudich, J. A., and Watt, S. (1971) *J. Biol. Chem. 246*, 4866−71.
28. Barden, J. A., and dos Remedios, C. G. (1984) *J. Biochem. 96*, 913−21.
29. Sawyer, W. H., Woodhouse, A. G., Czarnecki, J. J., and Blatt, E. (1988) *Biochemistry 27*, 7733−40.
30. Wagner, P. D., and Weeds, A. G. (1977) *J. Mol. Biol. 109*, 455−70.
31. Ueno, H., and Morita, F. (1984) *J. Biochem. 96*, 895−900.
32. Wikman-Coffelt, J., Srivastava, S., and Mason, D. T. (1979) *Biochimie 61*, 1309−14.
33. Lakowicz, J. R. (1983) *Principles of fluorescence spectroscopy*, Plenum Press, New York.
34. Weast, R. C. (1982) *CRC Handbook of Chemistry and Physics*, 63rd ed., CRC Press, Boca Raton, FL.
35. Kinosita, K. Jr., Kawato, S., and Ikegami, A. (1977) *Biophys. J. 20*, 289−305.
36. Kinosita, K., Jr., Kawato, S., and Ikegami, A. (1984) *Adv. Biophys. 17*, 147−203.
37. Mendelson, R. A., Morales, M. F., and Botts, J. (1973) *Biochemistry 12*, 2250−5.
38. Thomas, D. D., Seidel, J. C., Gergely, J., and Hyde, J. S. (1975) *J. Supramol. Struct. 3*, 376−90.
39. Adhikari, B. B., Somerset, J., Stull, J. T., and Fajer, P. G. (1999) *Biochemistry 38*, 3127−32.
40. Kinosita, K., Jr., Ikegami, A., and Kawato, S. (1982) *Biophys. J. 37*, 461−4.
41. Howard, E. C., Lindahl, K. M., Polnaszek, C. F., and Thomas, D. D. (1993) *Biophys. J. 64*, 581−93.
42. Huxley, A. F. (1974) *J. Physiol. (London) 243*, 1−43.
43. Highsmith, S., and Cooke, R. (1983) *Cell Muscle Motil. 4*, 207−37.
44. Curmi, P. M., Stone, D. B., Schneider, D. K., Spudich, J. A., and Mendelson, R. A. (1988) *J. Mol. Biol. 203*, 781−98.
45. Burgess, S. A., Walker, M. L., White, H. D., and Trinick, J. (1997) *J. Cell Biol. 139*, 675−81.
46. Smyczynski, C., and Kasprzak, A. A. (1997) *Biochemistry 36*, 13201−7.
47. Xiao, M., Li, H., Snyder, G. E., Cooke, R., Yount, R. G., and Selvin, P. R. (1998) *Proc. Natl. Acad. Sci. U.S.A. 95*, 15309−14.
48. Xu, J., and Root, D. D. (1998) *J. Struct. Biol. 123*, 150−61.
49. Palm, T., Sale, K., Brown, L., Li, H., Hambly, B., and Fajer, P. G. (1999) *Biochemistry 38*, 13026−13034.
50. Houdusse, A., Kalabokis, V. N., Himmel, D., Szent-Gyorgyi, A. G., and Cohen, C. (1999) *Cell 97*, 459−70.
51. Berger, C. L., Craik, J. S., Trentham, D. R., Corrie, J. E., and Goldman, Y. E. (1996) *Biophys. J. 71*, 3330−43.
52. Hopkins, S. C., Sabido-David, C., Corrie, J. E., Irving, M., and Goldman, Y. E. (1998) *Biophys. J. 74*, 3093−110.
53. Dominguez, R., Freyzon, Y., Trybus, K. M., and Cohen, C. (1998) *Cell 94*, 559−71.
54. Patterson, B., Ruppel, K. M., Wu, Y., and Spudich, J. A. (1997) *J. Biol. Chem. 272*, 27612−7.
55. Batra, R., Geeves, M. A., and Manstein, D. J. (1999) *Biochemistry 38*, 6126−34.
56. Kinose, F., Wang, S. X., Kidambi, U. S., Moncman, C. L., and Winkelmann, D. A. (1996) *J. Cell Biol. 134*, 895−909.
57. Fujita, H., Sugiura, S., Momomura, S., Omata, M., Sugi, H., and Sutoh, K. (1997) *J. Clin. Invest. 99*, 1010−5.
58. Rayment, I., Holden, H. M., Sellers, J. R., Fananapazir, L., and Epstein, N. D. (1995) *Proc. Natl. Acad. Sci. U.S.A. 92*, 3864−8.

59. Rayment, I., Rypniewski, W. R., Schmidt, B. K., Smith, R., Tomchick, D. R., Benning, M. M., Winkelmann, D. A., Wesenberg, G., and Holden, H. M. (1993) *Science 261*, 50−8.
60. Wells, A. L., Lin, A. W., Chen, L. Q., Safer, D., Cain, S. M., Hasson, T., Carragher, B. O., Milligan, R. A., and Sweeney, H. L. (1999) *Nature 401*, 505−8.
61. Raucher, D., and Fajer, P. G. (1994) *Biochemistry 33*, 11993−9.
62. Raucher, D., Fajer, E. A., Sar, C., Hideg, K., Zhao, Y., Kawai, M., and Fajer, P. G. (1995) *Biophys. J. 68*, 128S−133S, discussion 134S.
63. Thomas, D. D., Ramachandran, S., Roopnarine, O., Hayden, D. W., and Ostap, E. M. (1995) *Biophys. J. 68*, 135S−141S.
64. Ramachandran, S., and Thomas, D. D. (1999) *Biochemistry 38*, 9097−9104.
65. Howard, J., and Spudich, J. A. (1996) *Proc. Natl. Acad. Sci. U.S.A. 93*, 4462−4.
66. Uyeda, T. Q., Abramson, P. D., and Spudich, J. A. (1996) *Proc. Natl. Acad. Sci. U.S.A. 93*, 4459−64.
67. Tanaka, H., Kitamura, K., Iwane, A., and Yanagida, T. (2000) *Biophys. J. 78*, 3A.
68. Veigel, C., Coluccio, L. M., Jontes, J. D., Sparrow, J. C., Milligan, R. A., and Molloy, J. E. (1999) *Nature 398*, 530−3.
69. Xie, X., Harrison, D. H., Schlichting, I., Sweet, R. M., Kalabokis, V. N., Szent, G. A., and Cohen, C. (1994) *Nature 368*, 306−12.
70. Cordova, N. J., Ermentrout, B., and Oster, G. F. (1992) *Proc. Natl. Acad. Sci. U.S.A. 89*, 339−43.

BI010566F